# FREE VIBRATION ANALYSIS OF GRAPHENE-REINFORCED FGM MICROPLATES UNDER DIFFERENT BOUNDARY CONDITIONS

**Nguyen Van Loi, Chu Thanh Binh***

*Hanoi University of Civil Engineering, Hanoi, Vietnam*

*Corresponding author: binhct@huce.edu.vn

(Received: September 05, 2024; Revised: September 27, 2024; Accepted: October 12, 2024)

DOI: 10.31130/ud-jst.2024.523E

**Abstract -** This paper analyzes the free vibration of micro-sized plates placed on the Winkler-Pasternak elastic foundation. The microplate is made from functionally graded material (FGM) and reinforced with graphene nanoplatelets (GPLs). The properties of the new material (GPL-reinforced FGM) are determined using the Halpin-Tsai model and the rule of mixtures. The governing equation for the free vibration of the micro-sized plate on the elastic foundation is developed based on a four-variable plate theory, the modified couple stress theory, and the Rayleigh-Ritz approach. The solution is compared and validated against existing studies, followed by an investigation of the effects of various parameters (material parameters, size-dependent effect, boundary conditions, and foundation coefficients) on the natural frequency of the microplate.

**Key words -** Free vibration analysis; FGM microplate; elastic foundation; four-variable plate theory; Rayleigh-Ritz method.

## 1. Introduction

The use of nano/microstructures is increasingly widespread in fields such as electronics, automation, micro-electromechanical systems (MEMS), and nano-electromechanical systems (NEMS) [1, 2]. Micro-sized beams and plates are crucial elements of various microdevices, making research into the mechanical behaviors of such microstructures essential. In recent years, functionally graded materials (FGMs), which combine ceramic and metal constituents, have garnered significant attention from scientists worldwide [3-7] due to their outstanding properties, such as high strength, toughness, corrosion resistance, and durability under high temperatures. To further enhance their material properties, an FGM model reinforced with graphene platelets (GPLs) has been proposed in recent studies [8], representing a highly promising area of research. Therefore, this paper will focus on analyzing a GPL-reinforced FGM microplate structure.

Currently, two theory models frequently used in the analysis of microstructures are the modified strain gradient theory (MSGT) and the modified couple stress theory (MCST) [9]. Among these, the MCST model, introduced by Yang et al. [10], is notable for requiring only a single length-scale parameter to capture size effects. Based on this MCST, many researchers have developed various size-dependent models to address different small-scale problems. For example, utilizing the classical Kirchhoff theory and the MCST model, Jomehzadeh et al. [11] and Yin et al. [12] analyzed the natural frequencies of isotropic microplates. Similarly, Reddy and Berry [13] investigated the axisymmetric bending behaviors of circular FGM microplates using the MCST model. Using the Mindlin plate model and the MCST, the mechanical behaviors of microplates were conducted by Zhou and Gao [14] and Ke et al. [15]. Using a Navier-type solution, Nguyen et al. [9] examined the natural frequencies of simply-supported FGM microplates resting on elastic foundations using the four-variable refined plate theory. Until now, we can see that most studies have focused on microbeams/microplates made of isotropic materials, FGMs, or GPL-reinforced porous materials [16, 17]. However, the free vibration analysis for GPL-reinforced FGM microplates resting on an elastic foundation remains unexplored.

This paper focuses on the free vibration analysis of a micro-sized FGM plate reinforced by GPLs resting on a Winkler-Pasternak elastic foundation. The material properties of the novel composite (i.e., GPL-reinforced FGM) are estimated using the Halpin-Tsai model and the rule of mixture. Subsequently, the governing equations for the free vibration problem are formulated based on a four-variable refined plate theory (RPT4), the MCST model, and the Rayleigh-Ritz method. In the numerical analysis section, the influences of parameters such as material, boundary conditions, size-dependent effects, and foundation parameters on the natural frequencies of the microplates are examined in detail.

## 2. Microplate model, kinematic relations, energy expressions, and solution procedure

### *2.1. GPL-reinforced FGM microplate model*

Consider a rectangular micro-sized plate placed on a Winkler-Pasternak elastic foundation with dimensions $a$ (width), $b$ (length), and $h$ (thickness), as shown in Figure 1. Where, $K_w$ is the bending stiffness coefficient, and $K_s$ is the shear stiffness coefficient. The microplate is made of FGM (with a ceramic-rich upper surface and a metal-rich lower surface) and is reinforced by GPLs.

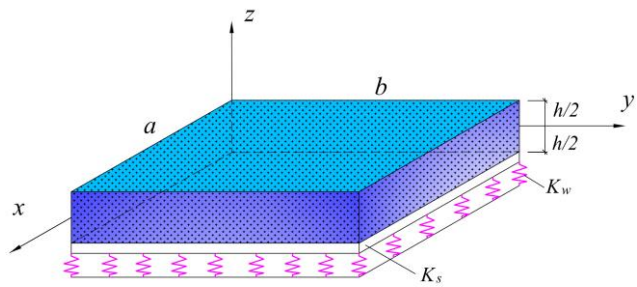


***Figure 1.*** *GPL-reinforced FGM microplate model placed on Winkler-Pasternak elastic foundation*

For the matrix material (FGM model), elastic Young's modulus, Poisson's ratio, and mass density are assumed to vary along the thickness with the following rule [18]:

$$E_M(z) = (E_c - E_m)\left(\frac{z}{h}+\frac{1}{2}\right)^p + E_m$$
$$\nu_M(z) = (\nu_c - \nu_m)\left(\frac{z}{h}+\frac{1}{2}\right)^p + \nu_m \quad (1)$$
$$\rho_M(z) = (\rho_c - \rho_m)\left(\frac{z}{h}+\frac{1}{2}\right)^p + \rho_m$$

Here, the subscripts "$m$" and "$c$" represent the quantities of the metal and ceramic components, respectively, and the parameter $p$ is the power-law index.

Based on the Halpin-Tsai model, the elastic Young's modulus, $E_c(z)$, of the composite (the GPL-reinforced FGM) is calculated as follows [19]:

$$E_c(z) = \frac{3}{8}\frac{1+\bar{\xi}_{11}\bar{\eta}_{11}V_{GPL}(z)}{1-\bar{\eta}_{11}V_{GPL}(z)}E_M + \frac{5}{8}\frac{1+\bar{\xi}_{22}\bar{\eta}_{22}V_{GPL}(z)}{1-\bar{\eta}_{22}V_{GPL}(z)}E_M \quad (2)$$

Parameters $\bar{\eta}_{11}$, $\bar{\eta}_{22}$, $\bar{\xi}_{11}$, and $\bar{\xi}_{22}$ is determined by

$$\bar{\eta}_{11} = \frac{E_{GPL}/E_M - 1}{E_{GPL}/E_M + \bar{\xi}_{11}}, \bar{\eta}_{22} = \frac{E_{GPL}/E_M - 1}{E_{GPL}/E_M + \bar{\xi}_{22}} \quad (3)$$

$$\bar{\xi}_{11} = 2(l_{GPL}/h_{GPL}), \bar{\xi}_{22} = 2(b_{GPL}/h_{GPL}) \quad (4)$$

Where $E_{GPL}$, $l_{GPL}$, $b_{GPL}$, and $h_{GPL}$ are the elastic Young's modulus, average length, width, and thickness of the GPL. For the composite material, the mass density $\rho_c(z)$ and Poisson's ratio $\nu_c(z)$ can be determined by the mixture principle [8]:

$$\rho_c(z) = \rho_{GPL}V_{GPL}(z) + \rho_M(z)[1 - V_{GPL}(z)]$$
$$\nu_c(z) = \nu_{GPL}V_{GPL}(z) + \nu_M(z)[1 - V_{GPL}(z)] \quad (5)$$

Here, $\rho_{GPL}$ and $\nu_{GPL}$ are the mass density and Poisson's ratio of the GPL, respectively. The GPL is assumed to be uniformly dispersed in the microplate, then $V_{GPL}(z)$ is calculated as follows [8]:

$$V_{GPL}(z) = \frac{W_{GPL}}{W_{GPL} + (1 - W_{GPL})\,\rho_{GPL}/\bar{\rho}_M} \quad (6)$$

In which, $W_{GPL}$ is the GPL weight fraction of the GPLs, and $\bar{\rho}_M = \frac{1}{h}\int_{-\frac{h}{2}}^{\frac{h}{2}}\rho_M(z)dz$.

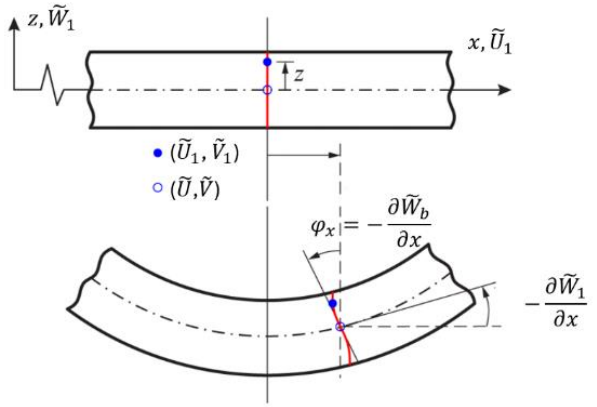


***Figure 2.*** *Displacement, deformation in the microplate*

### *2.2. Displacement components*

According to the RPT4 model, the displacement components in the microplate are defined as follows [20]:

$$\widetilde{U}_1(x,y,z,t) = \widetilde{U}(x,y,t) - z\widetilde{W}_{b,x} - f(z)\widetilde{W}_{s,x}; \quad (7)$$
$$\widetilde{V}_1(x,y,z,t) = \widetilde{V}(x,y,t) - z\widetilde{W}_{b,y} - f(z)\widetilde{W}_{s,y}; \quad (8)$$
$$\widetilde{W}_1(x,y,z,t) = \widetilde{W}_b(x,y,t) + \widetilde{W}_s(x,y,t); \quad (9)$$

In which $\widetilde{U}_1, \widetilde{V}_1$ and $\widetilde{W}_1$ are the three displacement components at a specific point in the microplate along the $x, y$, and $z$ directions of the coordinate system (Figure 2). $\widetilde{U}, \widetilde{V}$ are the two displacement components on the mid-surface along the $x$ and $y$ directions. $\widetilde{W}_b$ and $\widetilde{W}_s$ are the bending and shear components of the deflection $\widetilde{W}_1$. In this paper, the function $f(z) = -\frac{z}{8} + \frac{3}{2}\left(\frac{z^3}{h^2}\right)$ is selected for analysis [20].

### *2.3. Strain components*

The strain-displacement relations for the microplate, based on the RPT4 theory, are determined as follows:

$$\begin{Bmatrix}\varepsilon_{xx}\\ \varepsilon_{yy}\\ \gamma_{xy}\end{Bmatrix} = \boldsymbol{\varepsilon_0} + z\boldsymbol{\varepsilon_b} + f(z)\boldsymbol{\varepsilon_s}; \quad \begin{Bmatrix}\gamma_{yz}\\ \gamma_{xz}\end{Bmatrix} = g(z)\boldsymbol{\gamma_s}. \quad (10)$$

where $g(z) = 1 - f'(z)$ and

$$\boldsymbol{\varepsilon_0} = \begin{Bmatrix}\widetilde{U}_{,x}\\ \widetilde{V}_{,y}\\ \widetilde{U}_{,y} + \widetilde{V}_{,x}\end{Bmatrix}; \boldsymbol{\varepsilon_b} = \begin{Bmatrix}-\widetilde{W}_{b,xx}\\ -\widetilde{W}_{b,yy}\\ -2\widetilde{W}_{b,xy}\end{Bmatrix}; \quad (11)$$

$$\boldsymbol{\varepsilon_s} = \begin{Bmatrix}-\widetilde{W}_{s,xx}\\ -\widetilde{W}_{s,yy}\\ -2\widetilde{W}_{s,xy}\end{Bmatrix}; \boldsymbol{\gamma_s} = \begin{Bmatrix}\widetilde{W}_{s,y}\\ \widetilde{W}_{s,x}\end{Bmatrix}. \quad (12)$$

Based on the MCST, the components of the curvature tensor for the microplate are expressed as [9]:

$$\chi_{xx} = \chi^0_{xx} + (1 + f_{,z})\chi^1_{xx}; \quad \chi_{yy} = \chi^0_{yy} + (1 + f_{,z})\chi^1_{yy}; \ \chi_{zz} = 0. \quad (13)$$

$$\chi_{xy} = \chi^0_{xy} + (1 + f_{,z})\chi^1_{xy}; \quad \chi_{yz} = \chi^0_{yz} + f_{,zz}\chi^1_{yz}; \ \chi_{xz} = \chi^0_{xz} + f_{,zz}\chi^1_{xz}. \quad (14)$$

in which

$$\chi^0_{xx} = \widetilde{W}_{b,xy}; \ \chi^1_{xx} = \frac{1}{2}\widetilde{W}_{s,xy};$$
$$\chi^0_{yy} = -\widetilde{W}_{b,xy}; \ \chi^1_{yy} = -\frac{1}{2}\widetilde{W}_{s,xy};$$
$$\chi^0_{xy} = \frac{1}{2}(\widetilde{W}_{b,yy} - \widetilde{W}_{b,xx});$$
$$\chi^1_{xy} = \frac{1}{4}(\widetilde{W}_{s,yy} - \widetilde{W}_{s,xx}); \quad (15)$$
$$\chi^0_{yz} = \frac{1}{4}(\widetilde{V}_{,xy} - \widetilde{U}_{,yy}); \ \chi^1_{yz} = -\frac{1}{4}\widetilde{W}_{s,x};$$
$$\chi^0_{xz} = \frac{1}{4}(\widetilde{V}_{,xx} - \widetilde{U}_{,xy}); \ \chi^1_{xz} = \frac{1}{4}\widetilde{W}_{s,y};$$

### *2.4. Stress components*

The stress-strain relations in the microplate structure are determined by [18]:

$$\begin{Bmatrix}\sigma_{xx}\\ \sigma_{yy}\\ \sigma_{xy}\\ \sigma_{yz}\\ \sigma_{xz}\end{Bmatrix} = \mathbf{C}\begin{Bmatrix}\varepsilon_{xx}\\ \varepsilon_{yy}\\ \gamma_{xy}\\ \gamma_{yz}\\ \gamma_{xz}\end{Bmatrix}; \quad (16)$$

$$\begin{Bmatrix}m_{xx}\\ m_{yy}\\ m_{xy}\\ m_{yz}\\ m_{xz}\end{Bmatrix} = 2G_c l_0^2\begin{Bmatrix}\chi_{xx}\\ \chi_{yy}\\ \chi_{xy}\\ \chi_{yz}\\ \chi_{xz}\end{Bmatrix}; \quad (17)$$

Where $l_0$ is length scale parameter ($l_0 = 17{,}6 \times 10^{-6}m$), and non-zero coefficients of the matrix $\boldsymbol{C}$ are:

$$C_{11} = C_{22} = \frac{E_c(z)}{1-\nu_c(z)^2};$$
$$C_{12} = C_{21} = \frac{\nu_c(z)E_c(z)}{1-\nu_c(z)^2}; \quad (18)$$
$$C_{66} = C_{44} = C_{55} = G_c = \frac{E_c(z)}{2[1+\nu_c(z)]}.$$

### *2.5. Stress resultants*

The stress resultants in the microplate are defined as follows:

$$\left(N_i, M_i^b, M_i^s\right) = \int_{-h/2}^{h/2}\sigma_i(1, z, f)dz \quad (19)$$
$$i = xx, yy, xy;$$

$$Q_i = \int_{-h/2}^{h/2} g\sigma_j dz \; i = yz, xz; \quad (20)$$

$$P_i = \int_{-h/2}^{h/2} m_i dz \; i = xx, yy, xy, yz, xz; \quad (21)$$

$$R_i = \int_{-h/2}^{h/2}\left(1+f_{,z}\right)m_i dz \; i = xx, yy, xy; \quad (22)$$

$$S_i = \int_{-h/2}^{h/2} f_{,zz}m_i dz \; i = yz, xz; \quad (23)$$

### *2.6. Energy expressions*

The strain energy of the microplate (over the entire volume $V$) is defined by [21, 22]:

$$U = \frac{1}{2}\int_V\left(\sigma_{xx}\varepsilon_{xx} + \sigma_{yy}\varepsilon_{yy} + \sigma_{xy}\gamma_{xy} + \sigma_{yz}\gamma_{yz} + \sigma_{xz}\gamma_{xz} + m_{xx}\chi_{xx} + m_{yy}\chi_{yy} + 2m_{xy}\chi_{xy} + 2m_{yz}\chi_{yz} + 2m_{xz}\chi_{xz}\right)dV \quad (24)$$

The strain energy of the Winkler-Pasternak foundation is calculated by:

$$U_f = \frac{1}{2}\int_S\left\{K_w\widetilde{W}_1^2 + K_s\left[\widetilde{W}_{1,x}^2 + \widetilde{W}_{1,y}^2\right]\right\}dS \quad (25)$$

In which $S$ is the area of the mid-surface of the microplate. The kinetic energy of the microplate is determined by:

$$T = \frac{1}{2}\int_S\int_{-\frac{h}{2}}^{\frac{h}{2}}\rho_c(z)\left[\dot{\widetilde{U}}_1^2 + \dot{\widetilde{V}}_1^2 + \dot{\widetilde{W}}_1^2\right]dzdS \quad (26)$$

The total potential energy and total kinetic energy of the GPL-reinforced FGM microplate are determined by:

$$U_\Sigma = U + U_f; T_\Sigma = T; \quad (27)$$

### *2.7. Rayleigh-Ritz procedure*

For convenience, normalized coordinates $(\xi_1, \eta_1)$ are used instead of Cartesian coordinates $(x, y)$, as follows:

$$\xi_1 = \frac{2x}{a} - 1;\ \eta_1 = \frac{2y}{b} - 1; \quad (28)$$

With the pb2-Ritz functions, the displacement components of the microplate are assumed as follows [23, 24]:

$$\widetilde{U}(x,y,t) = \sum_{p=0}^{N^*}\sum_{r=0}^{p}A_j u_j(\xi_1,\eta_1)e^{i\omega t};$$
$$\widetilde{V}(x,y,t) = \sum_{p=0}^{N^*}\sum_{r=0}^{p}B_j v_j(\xi_1,\eta_1)e^{i\omega t};$$
$$\widetilde{W}_b(x,y,t) = \sum_{p=0}^{N^*}\sum_{r=0}^{p}C_j w_{bj}(\xi_1,\eta_1)e^{i\omega t}; \quad (29)$$
$$\widetilde{W}_s(x,y,t) = \sum_{p=0}^{N^*}\sum_{r=0}^{p}D_j w_{sj}(\xi_1,\eta_1)e^{i\omega t};$$

Where $\omega$ is the natural frequency of the system, $t$ is the time variable, and $i$ is the imaginary unit. $N^*$ is the order of the two-dimensional polynomial expansion. $\left(A_j, B_j, C_j, D_j\right)$ are the undetermined coefficients. The number of terms $M$ for $\left(A_j, B_j, C_j, D_j\right)$, and the index $j$ are calculated by:

$$M = \frac{(N^*+1)(N^*+2)}{2};$$
$$j = \frac{(p+1)(p+2)}{2} - (p-r); \quad (30)$$

Here, $\left(u_j, v_j, w_{bj}, w_{sj}\right)$ are the Ritz pb-2 functions, which are presented in Ref. [25]. By substituting the Eq. (29) into the displacement expressions of Eq. (27), the maximum total potential energy ($U_{max}$) and maximum total kinetic energy ($T_{max}$) of the microplate will be determined. The Lagrangian function of the microplate is defined as follows:

$$L = T_{max} - U_{max} \quad (31)$$

According to the Rayleigh-Ritz method, to determine the governing equation for the problem, the Lagrangian function $L$ is minimized with respect to the expansion coefficients of the series (29), that is [26, 27]:

$$\frac{\partial L}{A_j} = \frac{\partial L}{B_j} = \frac{\partial L}{C_j} = \frac{\partial L}{D_j} = 0, j = (1,2,\ldots M) \quad (32)$$

Finally, we obtain the governing equation of the problem written in matrix form as follows:

$$(K - \omega^2 M)q = 0. \quad (33)$$

In which $K$ and $M$ are the stiffness and mass matrices, respectively, and $q = \{A_1\ A_2\ \ldots A_M \ldots D_M\}^T$ is the coefficient vector. By solving equation (33), we obtain the natural frequencies and corresponding mode shapes of the microplate.

## 3. Numerical results

In the following sections, the FGM microplate model made from two constituent materials, $Al/ZrO_2$, with

material parameters $E_m = 70\ GPa, \rho_m = 2702\ kg/m^3, \nu_m = 0.3$ $(Al)$ and $E_c = 151\ GPa, \rho_c = 3000\ kg/m^3, \nu_c = 0.3$ $(ZrO_2)$. The FGM microplate is reinforced by GPLs with $E_{GPL} = 1010\ GPa, \rho_{GPL} = 1062.5\ kg/m^3, \nu_{GPL} = 0.186$ and $l_{GPL} = 3\ nm$; $b_{GPL} = 1.8\ nm$; $h_{GPL} = 0.7\ nm$. The rectangular microplate has four edges, and we conventionally name the boundary conditions in a counterclockwise sequence starting from the edge $y = 0$. For example, a microplate with the boundary condition CSCF indicates clamped (C) at $y = 0$, simply supported (S) at $x = a$, clamped (C) at $y = b$, and free (F) at $x = 0$. Additionally, for convenience, the following natural frequency parameters and elastic foundation coefficients are used in the analysis:

$$\bar{\omega} = 100\omega h\sqrt{\rho_c/E_c};$$
$$\bar{K}_w = \frac{K_w a^4}{D_m};\ \bar{K}_s = \frac{K_s a^2}{D_m}; \quad (34)$$
$$D_m = \frac{E_m h^3}{12(1-\nu_m^2)}.$$

### *3.1. Validation*

In this section, the convergence of the results is considered first. Then, to verify the theoretical model and the numerical solution of the paper, some special cases are compared.

***Table 1.*** *Convergence of fundamental frequency $\bar{\omega}$ of GPL-reinforced FGM microplate with and without elastic foundation*

| $(\bar{K}_w, \bar{K}_s)$ | $l_0/h$ | $N^*$ | | | |
|---|---|---|---|---|---|
| | | 4 | 5 | 6 | 7 |
| (0,0) | 0 | 5.5639 | 5.5638 | 5.5638 | 5.5638 |
| | 0.4 | 7.2667 | 7.2666 | 7.2666 | 7.2666 |
| | 1 | 12.9422 | 12.9422 | 12.9422 | 12.9422 |
| (50, 50) | 0 | 8.8553 | 8.8553 | 8.8553 | 8.8553 |
| | 0.4 | 10.0132 | 10.0132 | 10.0132 | 10.0132 |
| | 1 | 14.6615 | 14.6615 | 14.6615 | 14.6615 |

#### *3.1.1. Convergence study*

For the Rayleigh-Ritz method, we need to consider the convergence of the numerical results. The dimensionless fundamental natural frequency $\bar{\omega}$ of the GPL-reinforced FGM $(Al/ZnO_2)$ microplate placed on an elastic foundation is considered in this section. The microplate model with the SSSS boundary condition, the power-law index $p = 1$, the GPL uniformly dispersed across the thickness, and the GPL weight fraction $W_{GPL} = 1.5\%$, and plate dimensions $b/a = 1$, and $a/h = 50$ are selected for this investigation. We can see that when increasing $N^*$, the convergence of the fundamental frequency $\bar{\omega}$ of the microplate is shown in Table 1, where $N^*$ is the degree of the polynomial in Eq. (29). Both microplates with and without elastic foundation and both macroplate and microplate are considered by changing the parameters $(\bar{K}_w, \bar{K}_s)$ and the parameter $l_0/h$. It is clear that the fundamental frequency $\bar{\omega}$ of the microplate converges when $N^* \geq 5$ (convergence rate is quite fast). Therefore, $N^* = 7$ will be chosen to perform numerical investigations in the following sections.

#### *3.1.2. Validation of the natural frequency of the FGM microplates*

In this section, the dimensionless fundamental frequency $\tilde{\omega} = (\omega a^2/h)\sqrt{\rho_c/E_c}$ of FGM microplates made of $Al/Al_2O_3$ are compared with Thai and Kim [18]. The fundamental frequency $\tilde{\omega}$ of micro-sized FGM plates with different $l_0/h$ ratios and different $p$ indices are listed in Table 2, here the microplate is considered to be subjected to the SSSS boundary condition and has dimensions $b/a = 1, a/h = 20$. It is clear that the present results using the RPT4 theory, the MCST model and the Rayleigh-Ritz method are consistent with the results of Thai and Kim [18] using Reddy's third-order shear deformation theory model combined with the MCST and the Navier solution.

***Table 2.*** *A comparison of the fundamental frequency $\tilde{\omega}$ of the FGM microplates*

| $l_0/h$ | Source | Power-law index $p$ | | | |
|---|---|---|---|---|---|
| | | 0 | 1 | 5 | 10 |
| 0 | Thai and Kim [18] | 5.9199 | 4.5228 | 3.8884 | 3.7622 |
| | Present | 5.9199 | 4.5228 | 3.8884 | 3.7622 |
| 0,4 | Thai and Kim [18] | 7.6708 | 6.0756 | 5.0199 | 4.7488 |
| | Present | 7.6708 | 6.0758 | 5.0202 | 4.7490 |
| 1 | Thai and Kim [18] | 13.5545 | 11.1042 | 8.8286 | 8.1494 |
| | Present | 13.5545 | 11.1050 | 8.8296 | 8.1500 |

***Table 3.*** *A comparison of the natural frequency $\hat{\omega}$ of the GPL-reinforced isotropic macroplates*

| $a/h$ | Mode | Source | | |
|---|---|---|---|---|
| | | Jafari and Kiani [28] | Roun et al. [8] | Present |
| 20 | 1 | 0.0312 | 0.0312 | 0.0312 |
| | 2 | 0.0770 | 0.0769 | 0.0769 |
| | 3 | 0.1217 | 0.1215 | 0.1215 |
| | 4 | 0.1508 | 0.1505 | 0.1506 |
| 30 | 1 | 0.0139 | 0.0139 | 0.0139 |
| | 2 | 0.0346 | 0.0346 | 0.0346 |
| | 3 | 0.0550 | 0.0551 | 0.0551 |
| | 4 | 0.0686 | 0.0685 | 0.0686 |

#### *3.1.3. Validation of the natural frequency of the GPL-reinforced macroplates*

In this section, the dimensionless natural frequency $\hat{\omega} = \omega h\sqrt{\rho_m/E_m}$ of a GPL-reinforced isotropic macroplate are compared with those of Jafari and Kiani [28], who used quasi-3D theory, and with those of Roun et al. [8], who employed the RPT4 theory. Note that for the macroplate, the size effects are ignored. The plate is under the SSSS boundary condition with $b/a = 1$, and two cases, $a/h = 20$ and 30, are compared. Details of material parameters and input data based on reference [28]. It is observed that the present results are very close to those provided by Jafari and Kiani [28] and by Roun et al. [8] using the Navier-type analytical solution, as shown in Table 3.

Although there is no existing research on the GPL-reinforced FGM microplate model on the elastic foundation for validation, the specific cases above indicate that the theoretical model and solution presented in this

paper are highly reliable. This allows us to investigate the effects of material parameters, boundary conditions, size effects, and elastic foundation parameters on the natural frequency of the GPL-reinforced FGM microplate.

### *3.2. Parametric study*

#### *3.2.1. Effect of the GPL weight fraction*

In this section, the effect of the GPL weight fraction ($W_{GPL}$) on the fundamental frequency $\bar{\omega}$ of the microplate is presented. Figure 3 illustrates the variation of the fundamental frequency of the GPL-reinforced FGM microplate as $W_{GPL}$ increases from 0 to 3%, considering three boundary conditions: SSSS, CSCS, and CCCC. The microplate has parameters $b/a = 1, a/h = 50, \bar{K}_w = 0, \bar{K}_s = 0,$ the power-law index $p = 1$, and $h/l_0 = 1$ (with $l_0 = 17.6\,\mu m$).

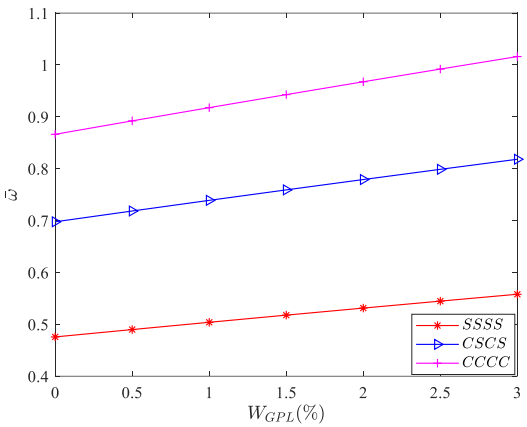


***Figure 3.*** *Variation of the fundamental frequency $\bar{\omega}$ of the microplate with respect to $W_{GPL}$*

It is observed that the dimensionless fundamental frequency $\bar{\omega}$ of the microplate steadily increases as the GPL content in the microplate rises, and this trend is consistent with all three boundary conditions: SSSS, CSCS, and CCCC, as shown in the figure. This is clearly due to the significantly higher stiffness of the GPLs compared to the FGM matrix, so even a small increase in the GPL content substantially raises the stiffness and fundamental frequency of the microplate. For example, when $W_{GPL} = 1.5\%$, the fundamental frequency $\bar{\omega}$ of the GPL-reinforced FGM microplate increases by approximately 8.8% (in all three boundary condition cases). When $W_{GPL} = 3\%$, the fundamental frequency $\bar{\omega}$ of the GPL-reinforced FGM microplate increases by about 17.3% (in all three boundary condition cases) compared to the case without GPL reinforcement.

#### *3.2.2. Effect of the boundary conditions*

In this section, the influence of the boundary conditions on the dimensionless fundamental frequency $\bar{\omega}$ of the GPL-reinforced FGM microplate is presented. Specifically, the fundamental frequency $\bar{\omega}$ of the microplate is calculated and shown in Figure 4 for four boundary conditions: SSSS, CSCS, CCCC, and CFCF. Here, the microplate under consideration has parameters $b/a = 1, a/h = 50, \bar{K}_w = 0, \bar{K}_s = 0,$ thickness-to-length ratio $h/l_0 = 1$ ($l_0 = 17.6\,\mu m$), and the GPL weight fraction $W_{GPL} = 1.5\%$.

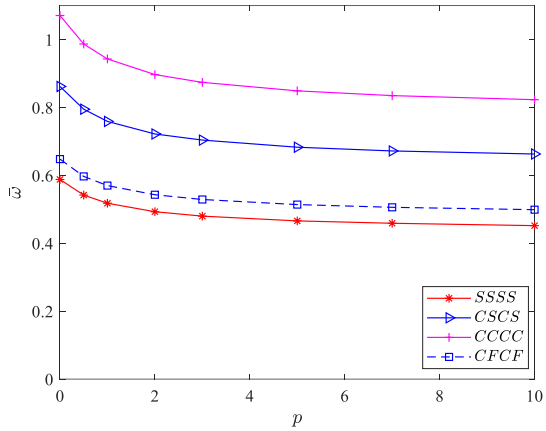


***Figure 4.*** *Variation of the fundamental frequency $\bar{\omega}$ of the GPL-reinforced FGM microplate with different boundary conditions*

It is evident that as the $p$ index increases, the fundamental frequency $\bar{\omega}$ of the microplate tends to change in a relatively similar manner across all four boundary conditions examined. Among these, the fundamental frequency of the microplate with the CCCC boundary condition is the highest, while that with the SSSS boundary condition is the lowest (in the cases investigated). This is because the CCCC boundary condition significantly enhances the stiffness of the microplate compared to the other cases. Additionally, as the volume fraction index increases, the microplates with SSSS and CCCC boundary conditions are slightly more affected (with a greater decrease) compared to the other cases.

#### *3.2.3. Effects of the power-law index and length scale parameter*

The influence of the power-law index ($p$) and length scale parameter ($\frac{h}{l_0}$) on the dimensionless fundamental frequency $\bar{\omega}$ of the GPL-reinforced microplate is evaluated in this section. Specifically, the microplate with the SSSS boundary condition and the parameters $\frac{b}{a} = 1$, $a/h = 50, \bar{K}_w = 0, \bar{K}_s = 0,$ and $W_{GPL} = 1.5\%$ is considered. The power-law index and length scale parameter are varied, and the results of this investigation are illustrated in Figure 5.

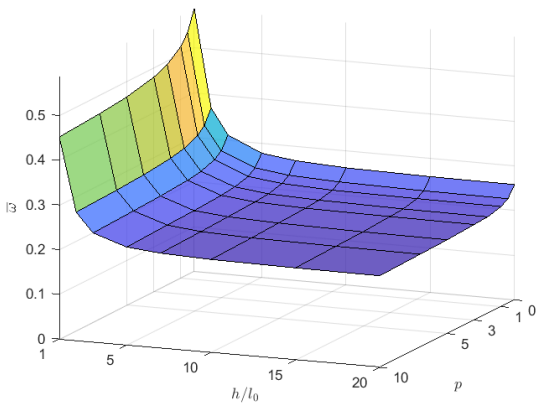


***Figure 5.*** *Variation of the fundamental frequency $\bar{\omega}$ of the microplates with respect to $p$ and $h/l_0$*

We can see that as the ratio $h/l_0$increases (increasing plate size), the fundamental frequency $\bar{\omega}$ of the microplate decreases sharply at first and then remains nearly constant in the later stage. When $h/l_0$ exceeds 10, the fundamental frequency $\bar{\omega}$ of the microplate changes minimally, indicating that larger microplates approach the behavior predicted by conventional macroplate. As the index $p$ increases (reducing the ceramic content), the fundamental frequency $\bar{\omega}$ of the microplate decreases. This effect occurs because the ceramic component is stiffer than the metallic component, so the stiffness of the microplate decreases as the ceramic content is reduced.

*3.2.4. Effect of the foundation parameters*

The influence of the foundation parameters $(\bar{K}_w, \bar{K}_s)$ on the dimensionless fundamental frequency $\bar{\omega}$ of the GPL-reinforced FGM microplate is illustrated in Figure 6. Here, the microplate with the SSSS boundary condition is considered, parameters $\frac{b}{a} = 1$, $\frac{a}{h} = 50$, $l_0/h = 1$ ($l_0 = 17.6\ \mu m$), $W_{GPL} = 1.5\ \%$, and the power-law index $p = 1$.

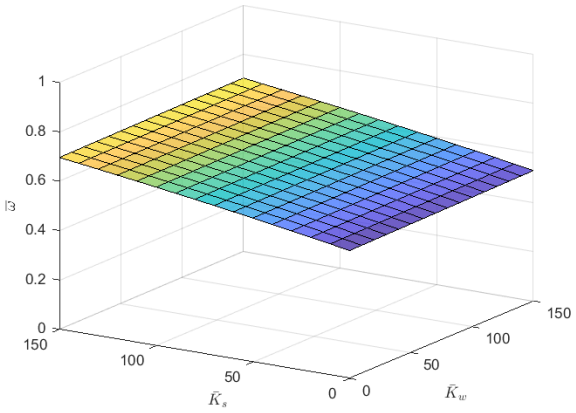


***Figure 6.*** *Variation of the fundamental frequency $\bar{\omega}$ of the microplate with respect to the parameters ($\bar{K}_w$, $\bar{K}_s$)*

Clearly, from the graph, it is evident that the elastic foundation parameter $\bar{K}_W$ has a minor effect on the fundamental frequency $\bar{\omega}$ of the GPL-reinforced FGM microplate. In comparison to the foundation parameter $\bar{K}_W$, the foundation parameter $\bar{K}_s$ has a more pronounced and significant impact on the fundamental frequency of the microplate.

## 4. Conclusion

The paper has analyzed the free vibration of the GPL-reinforced FGM microplates resting on a Winkler-Pasternak elastic foundation using the four-variable refined plate theory, the modified couple stress theory, and the Rayleigh-Ritz method. In the numerical analysis section, the effects of various factors, such as material parameters $(p, W_{GPL})$, size effects $(h/l_0)$, boundary conditions, and elastic foundation parameters $(\bar{K}_w, \bar{K}_s)$ on the fundamental frequency of the microplates have also been presented. Some key points to note from the research findings are:

- As the power-law index increases, the fundamental frequency of the GPL-reinforced FGM microplates decreases. Conversely, as the GPL weight fraction increases, the fundamental frequency of the microplate significantly increases.
- As the power-law index increases, the GPL-reinforced microplates with CCCC and SSSS boundary conditions experience slightly greater impacts than the other cases.
- As the ratio $h/l_0$ decreases (indicating smaller plate dimensions), the influence of the size dependency on the fundamental frequency of the microplate becomes more pronounced.
- The influence of the foundation parameter $\bar{K}_s$ is more pronounced than that of the foundation parameter $\bar{K}_w$ on the fundamental frequency of the microplates.

The analyses and observations in this study will be beneficial for scientists and engineers in the design and fabrication of microplate structures using the GPL-reinforced FGM model. Furthermore, potential directions for future research include calculating the behaviors of GPL-reinforced FGM microplates in hydrothermal environments, as well as analyzing the nonlinear mechanical behaviors of these microplates.

**Acknowledgments:** This research is funded by Ministry of Education and Training under grand number B2024.XDA.08.

## REFERENCES

[1] S. Tadigadapa and K. Mateti, "Piezoelectric MEMS sensors: state-of-the-art and perspectives", *Measurement Science and Technology*, vol. 20, p. 092001, 2009.

[2] C. Hierold, A. Jungen, C. Stampfer, and T. Helbling, "Nano electromechanical sensors based on carbon nanotubes", *Sensors and Actuators* A: Physical, vol. 136, pp. 51-61, 2007.

[3] D. K. Jha, T. Kant, and R. K. Singh, "A critical review of recent research on functionally graded plates", *Composite Structures*, vol. 96, pp. 833-849, 2013.

[4] H. T. Thai and S. E. Kim, "A review of theories for the modeling and analysis of functionally graded plates and shells", *Composite Structures*, vol. 128, pp. 70-86, 2015.

[5] V.-L. Nguyen, B.-D. Tran, and T.-B. Chu, "Free vibration analysis of functionally graded cylindrical shell with stiffeners", *Journal of Science and Technology in Civil Engineering (JSTCE) - HUCE*, vol. 12, no. 6, pp. 20-28, 2018. https://doi.org/10.31814/stce.nuce2018-12(6)-03.

[6] P. S. Ghatage, V. R. Kar, and P. E. Sudhagar, "On the numerical modelling and analysis of multi-directional functionally graded composite structures: A review", *Composite Structures*, vol. 236, p. 111837, 2020.

[7] T.-N. Nguyen, N.-D. Nguyen, and T.-K. Nguyen, "Development of Chebyshev-Ritz method for free vibration behavior of functionally graded material beams", *Journal of Science and Technology in Civil Engineering (JSTCE) - HUCE*, 2021. https://doi.org/10.31814/stce.huce(nuce)2022-16(1V)-07.

[8] S. Roun, V.-L. Nguyen, and J. Rungamornrat, "Free Vibration and Buckling Analyses of Functionally Graded Plates with Graphene Platelets Reinforcement", *Journal of Computing and Information Science in Engineering*, vol. 25, p. 011002, 2024.

[9] V.-L. Nguyen, X.-H. Dang, and Q.-C. Doan, "Free vibration of FGM microplates resting on elastic foundation", *Journal of Science and Technology in Civil Engineering (JSTCE) - HUCE*, vol. 18, pp. 34–47, 2024. https://doi.org/10.31814/stce.huce2024-18(3V)-03.

[10] F. Yang, A. C. M. Chong, D. C. C. Lam, and P. Tong, "Couple stress based strain gradient theory for elasticity", *International Journal of*

*Solids and Structures*, vol. 39, pp. 2731-2743, 2002/05/01/ 2002.

[11] E. Jomehzadeh, H. R. Noori, and A. R. Saidi, "The size-dependent vibration analysis of micro-plates based on a modified couple stress theory", *Physica E: Low-dimensional Systems and Nanostructures*, vol. 43, pp. 877-883, 2011/02/01/ 2011.

[12] L. Yin, Q. Qian, L. Wang, and W. Xia, "Vibration analysis of microscale plates based on modified couple stress theory", *Acta Mechanica Solida Sinica*, vol. 23, pp. 386-393, 2010/10/01/ 2010.

[13] J. N. Reddy and J. Berry, "Nonlinear theories of axisymmetric bending of functionally graded circular plates with modified couple stress", *Composite Structures*, vol. 94, pp. 3664-3668, 2012/12/01/ 2012.

[14] S.-S. Zhou and X.-L. Gao, "A Nonclassical Model for Circular Mindlin Plates Based on a Modified Couple Stress Theory", *Journal of Applied Mechanics*, vol. 81, 2014.

[15] L.-L. Ke, Y.-S. Wang, J. Yang, and S. Kitipornchai, "Free vibration of size-dependent Mindlin microplates based on the modified couple stress theory", J*ournal of Sound and Vibration*, vol. 331, pp. 94-106, 2012/01/02/ 2012.

[16] H.-T. Thai, T. P. Vo, T.-K. Nguyen, and S.-E. Kim, "A review of continuum mechanics models for size-dependent analysis of beams and plates", *Composite Structures*, vol. 177, pp. 196-219, 2017/10/01/ 2017.

[17] K. Yee and M. H. Ghayesh, "A review on the mechanics of graphene nanoplatelets reinforced structures", *International Journal of Engineering Science*, vol. 186, p. 103831, 2023/05/01/ 2023.

[18] H.-T. Thai and S.-E. Kim, "A size-dependent functionally graded Reddy plate model based on a modified couple stress theory", *Composites Part B: Engineering*, vol. 45, pp. 1636-1645, 2013/02/01/ 2013.

[19] S. Zhao, Z. Zhao, Z. Yang, L. Ke, S. Kitipornchai, and J. Yang, "Functionally graded graphene reinforced composite structures: A review", *Engineering Structures*, vol. 210, p. 110339, 2020/05/01/ 2020.

[20] H.-Q. Tran, V.-T. Vu, and M.-T. Tran, "Free vibration analysis of piezoelectric functionally graded porous plates with graphene platelets reinforcement by pb-2 Ritz method", *Composite Structures*, vol. 305, p. 116535, 2023/02/01/ 2023.

[21] H.-T. Thai and D.-H. Choi, "A refined plate theory for functionally graded plates resting on elastic foundation", *Composites Science and Technology*, vol. 71, pp. 1850-1858, 2011/11/14/ 2011.

[22] M. Şimşek and M. Aydın, "Size-dependent forced vibration of an imperfect functionally graded (FG) microplate with porosities subjected to a moving load using the modified couple stress theory", *Composite Structures*, vol. 160, pp. 408-421, 2017/01/15/ 2017.

[23] C. W. Lim and K. M. Liew, "A pb-2 Ritz formulation for flexural vibration of shallow cylindrical shells of rectangular planform", *Journal of Sound and Vibration*, vol. 173, pp. 343-375, 1994.

[24] L. H. Wu and Y. Lu, "Free vibration analysis of rectangular plates with internal columns and uniform elastic edge supports by pb-2 Ritz method", *International Journal of Mechanical Sciences*, vol. 53, pp. 494-504, 2011/07/01/ 2011.

[25] V.-L. Nguyen, V.-L. Nguyen, T.-A. Nguyen, and M.-T. Tran, "Dynamic responses of saturated functionally graded porous plates resting on elastic foundation and subjected to a moving mass using pb2-Ritz method", *Acta Mechanica*, 2024/06/14 2024.

[26] V.-L. Nguyen, S. Limkatanyu, H.-T. Thai, and J. Rungamornrat, "Simple First-order Shear Deformation Theory for Free Vibration of FGP-GPLRC Spherical Shell Segments", *Mechanics of Advanced Materials and Structures*, 2023.

[27] V.-L. Nguyen, S. Limkatanyu, T. Q. Bui, and J. Rungamornrat, "Free vibration analysis of rotating stiffened functionally graded graphene-platelet-reinforced composite toroidal shell segments with novel four-unknown refined theories", *International Journal of Mechanics and Materials in Design*, vol. 19, pp. 319–350, 2023/06/01 2023.

[28] P. Jafari and Y. Kiani, "Free vibration of functionally graded graphene platelet reinforced plates: A quasi 3D shear and normal deformable plate model", *Composite Structures*, vol. 275, p. 114409, 2021/11/01/ 2021.